Published in final edited form as:
Biochemistry. 2008 November 25; 47(47): 12260–12269. doi:10.1021/bi801683k.

Molecular Mechanism of an Oncogenic Mutation That Alters Membrane Targeting: Glu17Lys Modifies the PIP Lipid Specificity of the AKT1 PH Domain†

Kyle E. Landgraf, **Carissa Pilling**, and **Joseph J. Falke***
Department of Chemistry and Biochemistry and Molecular Biophysics Program, University of Colorado, Boulder, Colorado 80309-0215

Abstract

The protein kinase AKT1 regulates multiple signaling pathways essential for cell function. Its N-terminal PH domain (AKT1 PH) binds the rare signaling phospholipid phosphatidylinositol 3,4,5-trisphosphate [PI(3,4,5)P_3], resulting in plasma membrane targeting and phosphoactivation of AKT1 by a membrane-bound kinase. Recently, it was discovered that the Glu17Lys mutation in the AKT1 PH domain is associated with multiple human cancers. This mutation constitutively targets the AKT1 PH domain to the plasma membrane by an unknown mechanism, thereby promoting constitutive AKT1 activation and oncogenesis. To elucidate the molecular mechanism underlying constitutive plasma membrane targeting, this work compares the membrane docking reactions of the isolated wild-type and E17K AKT1 PH domains. In vitro studies reveal that the E17K mutation dramatically increases the affinity for the constitutive plasma membrane lipid PI(4,5)P_2. The resulting PI(4,5)P_2 equilibrium affinity is indistinguishable from that of the standard PI(4,5)P_2 sensor, PLCδ1 PH domain. Kinetic studies indicate that the effects of E17K on PIP lipid binding arise largely from electrostatic modulation of the dissociation rate. Membrane targeting analysis in live cells confirms that the constitutive targeting of E17K AKT1 PH to plasma membrane, like PLCδ1 PH, stems from PI(4,5)P_2 binding. Overall, the evidence indicates that the molecular mechanism underlying E17K oncogenesis is a broadened target lipid selectivity that allows high-affinity binding to PI(4,5)P_2. Moreover, the findings strongly implicate the native Glu17 side chain as a key element of PIP lipid specificity in the wild-type AKT1 PH domain. Other PH domains may employ an analogous anionic residue to control PIP specificity.

Many cellular signaling processes are controlled by events occurring at the surface of intracellular membranes. Phosphatidylinositiol phosphates (PIPs) comprise an important class of signaling phospholipids that are highly regulated second messengers and can drive the reversible localization of key signaling proteins from the cytoplasm to the inner leaflet of the plasma membrane (1–5). Such PIP-dependent localization events play essential roles in many signaling pathways. For example, on the cytoplasmic surface of the plasma membrane, the phosphatidylinositol 3-kinase (PI3K) family of lipid kinases convert a constitutive PIP lipid, phosphatidylinositol 4,5-bisphosphate [PI(4,5)P_2],[1] into the rare second-messenger lipid phosphatidylinositol 3,4,5-trisphosphate [PI(3,4,5)P_3] (1,6,7). This second messenger, in turn, recruits a wide array of important downstream protein effectors

†Supported by NIH Grant R01 GM-063235 (to J.J.F.) and by a grant from CU/HHMI Undergraduate Research Opportunities Program (to C.P.) and by funding from the NIH/CU Molecular Biophysics Training Program, supported in part by NIH T32 GM065103 (to K.L.).

*To whom correspondence should be addressed. falke@colorado.edu. Telephone: (303) 492-3503. Fax: (303) 492-5894.

containing pleckstrin homology (PH) domains that specifically bind to the PI(3,4,5)P_3 headgroup (8–10). The resulting plasma membrane targeting activates signaling proteins that are brought into the proximity of their membrane-associated substrate and effector lipids and proteins. Such PIP-specific membrane targeting provides exquisite spatiotemporal control of signaling events and represents a fundamental mechanism used by cells to organize signaling complexes and pathways.

The most extensively studied PH domain-regulated signaling circuit is the PI3K/PDK/AKT pathway known to be essential for normal cell motility, proliferation, growth, metabolism, and cell survival (11–13). In addition to the lipid kinase PI3K, the pathway consists of two PH domain-containing protein kinases, phosphoinositide-dependent kinase 1 (PDK1) and protein kinase B (AKT1). The pathway is downregulated by the well-known tumor suppressor PTEN (phosphatase and tensin homologue), a lipid phosphatase that degrades PI(3,4,5)P_3 (14). By contrast, due to the importance of the PI3K/PDK/AKT pathway in cell growth and survival, constitutive activation of the AKT1 protein kinase often causes oncogenesis and cancer (15). Recently, a novel mechanism of oncogenic AKT1 activation was discovered: the E17K mutation, located in the AKT1 PH domain near its PI(3,4,5)P_3-specific binding site, was found to cause constitutive AKT1 targeting to the plasma membrane, thereby yielding an elevated level of phosphoactivation of the AKT1 kinase domain by the membrane-bound kinase PDK1 (16). This E17K mutation has been linked to human breast, colorectal, ovarian, and lung cancers (16,17). Here we examine the molecular mechanism by which the E17K mutation drives the enhanced plasma membrane targeting that underlies pathological activation and oncogenesis.

The AKT1 PH domain, located at the N-terminus of full-length AKT1, has been successfully isolated, and its high-resolution structure has been determined in complex with inositol 1,3,4,5-tetrakisphosphate (IP_4), the soluble headgroup analogue of its target lipid PI(3,4,5)P_3 (16,18). This PH domain exhibits the canonical seven-strand β-sandwich core of the PH superfamily, where one edge of the core is stabilized by a rigid C-terminal α-helix and the opposite edge provides the variable interstrand loops that form the specific binding pocket for the PI(3,4,5)P_3 headgroup. Several key basic residues in the binding pocket dominate headgroup recognition, yielding strong interactions with the phosphate at the 3-position of the inositol ring that are critical for specific, tight binding (18,19). Since the plasma membrane of resting cells contains very low levels of PIP lipids phosphorylated at the inositol 3-position, the AKT1 PH domain possesses no appreciable plasma membrane affinity until activated PI3K phosphorylates PI(4,5)P_2 to generate PI(3,4,5)P_3 (20,21). The resulting PI(3,4,5)P_3 signal recruits both the AKT1 and PDK1 PH domains to the plasma membrane, thereby stimulating PDK1 phosphoactivation of AKT1. Following phosphorylation at T308, the membrane-docked AKT1 kinase can modify membrane-bound substrate proteins or can dissociate from PI(3,4,5)P_3 and modify cytoplasmic substrates (22,23).

At least two models can be proposed for the molecular mechanism by which the E17K mutation drives constitutive targeting of the AKT1 PH domain to the plasma membrane. In principle, the charge reversal introduced by the Glu to Lys substitution could cause a sufficient increase in PI(3,4,5)P_3 affinity to drive recruitment of the mutant PH domain to the very low, basal level of PI(3,4,5)P_3 present in the resting plasma membrane. Alternatively, E17K could alter the PIP lipid specificity of AKT1 PH domain in a way that

[1]Abbreviations: AKT1, protein kinase B, isoform 1; PDK1, phos-phoinositide-dependent protein kinase 1; PLCδ1, phospholipase Cδ, isoform 1; PH, pleckstrin homology; PC, phosphatidylcholine; PS, phosphatidylserine; PE, phosphatidylethanolamine; dPE, dansyl-PE; PI(3,4,5)P_3, phosphatidylinositol 3,4,5-trisphosphate; PI(4,5)P_2, phosphatidylinositol 4,5-bisphosphate; DTT, dithiothreitol; IP_6, inositol hexakisphosphate.

allows binding to the more prevalent $PI(4,5)P_2$ that is constitutively present in the plasma membrane. Ultimately, identification of the membrane targeting mechanism of the E17K mutation is critical to the understanding of its unregulated membrane recruitment and oncogenesis.

To directly ascertain the molecular mechanism of altered membrane recruitment, this study investigates the effects of E17K on the equilibrium and kinetics of binding of the AKT1 PH domain to $PI(4,5)P_2$ and $PI(3,4,5)P_3$ embedded in membranes that mimic the plasma membrane inner leaflet (24). These quantitative studies indicate that the constitutive targeting of the mutant AKT1 E17K PH domain stems primarily from an increased affinity for $PI(4,5)P_2$. Live cell fluorescence imaging studies confirm that the AKT1 E17K PH domain colocalizes with the PLCδ1 PH domain, a biomarker for $PI(4,5)P_2$ (25,26), at the plasma membrane and dissociates from the membrane upon $PI(4,5)P_2$ hydrolysis. Together, these in vitro and live cell studies directly demonstrate that the E17K mutation alters the PIP lipid specificity of the AKT1 PH domain, allowing high-affinity binding to the constitutive $PI(4,5)P_2$ population of the plasma membrane even in the absence of a $PI(3,4,5)P_3$ signal. At the same time, the findings strongly implicate the native Glu17 residue as a central player in defining the PIP lipid specificity of the wild-type AKT1 PH domain.

MATERIALS AND METHODS

Reagents

All lipids were synthetic unless otherwise indicated. 1-Palmitoyl-2-oleoyl-*sn*-glycero-3-phosphocholine (phosphatidylcholine, POPC, PC), 1-palmitoyl-2-oleoyl-*sn*-glycero-3-phosphoethanolamine (phosphatidylethanolamine, POPE, PE), 1-palmitoyl-2-oleoyl-*sn*-glycero-3-phosphoserine (phosphatidylserine, POPS, PS), L-α-phosphatidylinositol (17) natural from bovine liver, L-α-phosphatidylinositol 4,5-bisphosphate [$PI(4,5)P_2$, PIP_2] natural from porcine brain, and sphingomyelin (15) natural from brain were all purchased from Avanti Polar Lipids. 1,2-Dipalmitoylphosphatidylinositol 3,4,5-trisphosphate [phosphatidylinositol 3,4,5-trisphosphate, $PI(3,4,5)P_3$] was from Cayman Chemical. *N*-[5-(Dimethylamino)naphthalene-1-sulfonyl]-1,2-dihexadecanoyl-*sn*-glycero-3-phosphoethanolamine (dansyl-PE, dPE) was from Molecular Probes. Cholesterol (CH), inositol 1,2,3,4,5,6-hexakisphosphate (IP_6), and wortmannin were from Sigma. Lipofectamine 2000 transfection reagent was from Invitrogen. Human recombinant PDGF-BB was purchased from PeproTech.

Preparation of PH Domains

For in vitro binding studies, the PH domains of human AKT1 (IMAGE clone 4562823, residues 1–120) and mouse PLCδ1 (IMAGE clone 2136830, residues 12–142) were cloned by PCR into the EcoRI–XbaI site of a previously described glutathione *S*-transferase (GST) fusion vector (27). Mutagenesis of the AKT1 PH domain to generate E17K and E17Q was carried out using a Quick-ChangeXLII site-directed mutagenesis kit (Stratagene). The GST fusion constructs were overexpressed in BL21 *Escherichia coli* cells and isolated on a glutathione affinity column as previously described (27).

Preparation of Lipid Mixtures and Phospholipid Vesicles

Phospholipid bilayer vesicles were created using three lipid compositions (see Table 1 below) to mimic the plasma membrane inner leaflet either lacking or containing a PIP lipid: PM(−)PIP, PM(+)$PI(4,5)P_2$, and PM(+)$PI(3,4,5)P_3$. Lipids were dissolved in a chloroform/methanol/water mixture (1/2/0.8), dried under vacuum until all solvents were removed, and then hydrated by being vortexed with binding buffer [25 mM *N*-(2-hydroxyethyl)piperazine-*N*′-2-ethane-sulfonic acid (HEPES) (pH 7.4) with KOH, 140 mM KCl, 15 mM NaCl, and

0.5 mM $MgCl_2$]. Sonicated unilamellar phospholipid vesicles (SUVs) were prepared using a Misonix XL2020 probe sonicator as previously described (24,27), yielding a total lipid concentration of 3 mM.

Fluorescence Spectroscopy

Equilibrium binding experiments were conducted on a Photon Technology International QM-2000-6SE fluorescence spectrometer at 25 °C in binding buffer (above) with 10 mM dithiothreitol (DTT). Excitation and emission slits were 1 and 8 nm, respectively.

Qualitative Analysis of PIP Lipid Specificity

Qualitative analysis of the binding of the PH domain to membrane-embedded PIP lipids was carried out by mixing 0.5 μM free PH domain with 50 μM total lipid in binding buffer with 10 mM DTT, yielding an equimolar ratio of protein to accessible PIP_n lipid for the PM(+)PIP_n mixtures. Subsequently, the relative intensity of protein-to-membrane FRET for each mixture (Figure 1) was measured as previously described (27).

Quantitative Measurement of PIP Lipid Affinity and Specificity

A previously described competitive displacement assay was used to quantitate the high-affinity binding of each PH domain to the selected PIP lipids (27). In this approach, soluble inositol 1,2,3,4,5,6-hexakisphosphate (IP_6) is employed as a competitive inhibitor. [The isolated headgroups of PI(3,4,5)P_3 and PI(4,5)P_2, IP_4, and IP_3 are not suitable competitive inhibitors because they bind too tightly to the free AKT1 PH domain or to the E17K mutant to quantitate their affinities, while the lower affinity of IP_6 is in an ideal range for measurement.] First, the affinity of the free PH domain for IP_6 is measured, using an increase in intrinsic Trp fluorescence to monitor binding of IP_6 to the protein. Second, the IP_6 is titrated into a sample containing the PH domain bound to a membrane-associated PIP lipid, using a protein-to-membrane FRET assay to monitor the membrane-bound PH domain. The IP_6 competitively displaces the PH domain from the membrane, yielding a decrease in the extent of FRET. Finally, nonlinear least-squares curve fits to standard binding equations are used to determine the equilibrium dissociation constant for IP_6 binding to the PH domain [$K_D(IP_6)$], the equilibrium inhibition constant for IP_6, displacement of the PH domain from PIP lipid [$K_D(IP_6)_{app}$], and the desired equilibrium dissociation constant for the binding of the PH domain to the membrane-associated PIP lipid [$K_D(PIP_n)$]. All procedures were carried out in binding buffer with 10 mM DTT as previously described, except that the Trp fluorescence wavelengths employed in IP_6 binding measurements were optimized for the relevant PH domains: λ_{ex} = 284 nm, λ_{em} = 322 nm for the AKT1 PH domain, and λ_{em} = 340 nm for the PLCδ1 PH domain. Changes in binding free energies ($\Delta\Delta G$) were calculated from the standard relationship [$\Delta\Delta G = -RT \ln(K_{D2}/K_{D1})$] and expressed in units of thermal energy (RT).

Quantitative Measurement of Association and Dissociation Kinetics

All kinetic experiments were carried out using Applied Photophysics SX.17 stopped-flow fluorescence instrument to monitor changes in protein-to-membrane FRET induced by membrane association or dissociation, always in binding buffer with 10 mM DTT, at 25 °C. Association kinetics were measured by rapidly mixing the PH domain (0.5 μM) with SUVs (200 μM total lipid) containing excess PIP_n target lipid (3 μM accessible). Under these conditions, the forward binding reaction is virtually irreversible due to the high affinity of the PH domain for PIP lipid, and best fit analysis of the binding time course with a double exponential yields a predominant, fast component used to calculate the on-rate constant (k_{on}) as previously described (27). Dissociation kinetics were measured by rapidly mixing the preformed, PH domain–membrane complex (0.5 μM protein and 200 μM total lipid) with

excess IP_6 (40 mM). Best fitting of a single-exponential function to the dissociation time course yields the off-rate constant (k_{off}) as previously described (27). The dissociation of the AKT1 E17K PH domain from membranes containing $PI(3,4,5)P_3$ displayed biphasic behavior best fit with a double-exponential function, and the highly reproducible, slow component was used to calculate the off-rate constant.

Fluorescent Fusion Proteins

The E17K and wild-type AKT1 PH domains were subcloned from the previously described EGFP–AKT1 PH construct (28) into the pmR-FP(C3) and pmCitrine(C3) vectors (Clontech), yielding fusion proteins possessing an N-terminal fluorescent protein: RFP–AKT1 E17K PH and Citrine–AKT1 PH. pECFP-PLCδ1 PH was a gift from M. Katan (Cancer Research UK Centre for Cell and Molecular Biology, London, U.K.).

Transfections into Live Cells

NIH 3T3 cells (American type Culture Collection) were cultured in DMEM containing 10% fetal bovine serum, 100 units/mL penicillin, 100 μg/mL streptomycin, and 0.292 mg/mL glutamine in 5% CO_2 at 37 °C. Cells were plated in 35 mm glass bottom dishes (MatTek) at a density of 1×10^5 cells/dish, and transfections were carried out with 3 μg of total DNA using lipofectamine 2000 (Invitrogen) with OptiMEM (Invitrogen) according to the manufacturer's protocol. Where indicated, serum starvation of cells was carried out in DMEM containing 0.2% BSA and 0.292 mg/mL glutamine and incubated for 6 h in 5% CO_2 at 37 °C.

Cell Imaging Studies

Cotransfected NIH 3T3 cells were rinsed and incubated in HBSS buffered with 25 mM HEPES (pH 7.4) (HHBSS) containing 0.01% endotoxin-free BSA. When Ca^{2+}-stimulated $PI(4,5)P_2$ hydrolysis was carried out, the buffer also contained 3 mM EGTA to provide an initial, Ca^{2+}-free extracellular environment. Simultaneous CFP, Citrine, and RFP images were acquired on a Nikon inverted microscope equipped with a 60× 1.4 NA oil immersion objective, a CFP/YFP-Citrine/RFP dichroic mirror, singleband excitation and emission filters (Chroma Technology), a CoolSNAP ES camera (Photometrics), and a mercury lamp. For the kinetic time courses, time-lapse imaging involved 300 ms acquisitions of CFP, Citrine, and RFP with a total of 10 or 5 s between image sets for PDGF or Ca^{2+} studies, respectively. Images were produced in ImageJ (National Institutes of Health, Bethesda, MD).

RESULTS

Strategy

Recent studies of the oncogenic E17K mutant of AKT1 have provided strong evidence that its carcinogenicity arises from the constitutive plasma membrane targeting of the mutant PH domain (16). To understand the molecular basis of E17K-triggered carcinogenicity, it is crucial to determine the mechanism of altered targeting. Our initial, qualitative studies indicate that the E17K mutation broadens the PIP lipid specificity of the PH domain, enabling high-affinity binding to $PI(4,5)P_2$ as well as $PI(3,4,5)P_3$. Further in vitro studies quantify the effect of the E17K mutation on the equilibrium and kinetics of the AKT1 PH domain docking to both of these PIP lipids embedded in a lipid bilayer we term the "synthetic plasma membrane" because it closely mimics the lipid composition of the plasma membrane inner leaflet (Table 1; note this synthetic version lacks leaflet asymmetry and all nonlipid components of the plasma membrane). Finally, the PIP lipid selectivity determined in vitro is tested by membrane targeting studies in live cells. Together, the in vitro and live

cell findings clearly define the molecular basis of the targeting defect caused by the E17K mutation.

Qualitative Analysis of PIP Lipid Selectivities

To analyze the PIP lipid specificities of native and mutant AKT1 PH domains, we employed a protein-to-membrane FRET assay previously developed in our laboratory to monitor the docking of peripheral proteins to membranes (27). In this assay, one or more of the intrinsic tryptophan residues in the PH domain (four for AKT1 PH and three for PLCδ1 PH) serve as FRET donors, and a low density of membrane-embedded, dansyl-PE lipids serve as acceptors. Each PH domain was added to synthetic plasma membranes containing an equimolar amount of accessible $PI(4,5)P_2$ or $PI(3,4,5)P_3$, and the relative increase in the level of FRET was measured.

Figure 1 compares the qualitative PIP lipid selectivity patterns of the native PH domain (WT), the E17K charge reversal mutant, and the E17Q charge neutralization mutant. Strikingly, relative to the WT domain, E17K increases the protein-to-membrane FRET for binding to $PI(4,5)P_2$-containing membranes by ~1 order of magnitude (where this enhancement is quantified by subtracting the background signal defined by membranes lacking PIPs). By contrast, E17Q exhibits a smaller, intermediate-affinity enhancement for $PI(4,5)P_2$, supporting the idea that the observed effects of mutagenesis at the E17 position are dominated by electrostatics. No detectable changes to $PI(3,4,5)P_3$ binding are observed, since high-affinity binding to this lipid is essentially saturated at the concentrations of the PH domain and target $PI(3,4,5)P_3$ employed (Figure 1). Overall, these initial qualitative findings indicate that the E17K mutation significantly increases the affinity for $PI(4,5)P_2$ but cannot resolve whether altered plasma membrane targeting arises from the increased affinity for $PI(3,4,5)P_3$ or $PI(4,5)P_2$. To better address this issue, we also carried out quantitative measurements of the effect of E17K on AKT1 PH domain affinities for both $PI(3,4,5)P_3$ and $PI(4,5)P_2$.

Quantification of PIP Lipid Affinities and Selectivities

To quantify the binding of PH domains to their membrane-bound target PIP lipids, we recently developed a competitive displacement assay suitable for measuring nanomolar PIP lipid affinities (27). The approach begins with the PH domain bound to its target lipid embedded in synthetic plasma membranes and uses protein-to-membrane FRET to monitor the displacement of the domain as the competitive inhibitor inositol hexakisphosphate (IP_6) is titrated into the sample, yielding an apparent inhibitor affinity [$K_I(IP_6)$]. Subsequently, the IP_6 affinity of the free PH domain [$K_D(IP_6)$] is determined independently by titrating the domain with IP_6 while monitoring the IP_6-induced change in the intrinsic tryptophan fluorescence. Finally, a standard competition binding equation describing the effect of a competitive inhibitor on the apparent dissociation constant is used to quantitatively define the affinity of the PH domain for the target lipid PIP_n [$K_D(PIP_n)$].

We applied this method to the WT and E17K AKT1 PH domains and to the PLCδ1 PH domain, yielding their equilibrium affinities for both $PI(3,4,5)P_3$ and $PI(4,5)P_2$. The WT AKT1 PH domain is known to preferentially bind $PI(3,4,5)P_3$, while the PLCδ1 PH domain is specific for $PI(4,5)P_2$ (18,19,25); thus, these domains are useful as internal controls in the determination of the unknown specificity of the E17K AKT1 PH domain. Figure 2A–C displays the resulting IP_6 binding curves for the free domains, while Figure 2D–F shows the IP_6 competitive displacement curves for the same domains bound to target PIP_n lipid on a synthetic plasma membrane surface. For each titration curve, the best fit $K_D(IP_6)$ or $K_I(IP_6)$ value was determined by nonlinear least-squares fitting to the appropriate equation for a homogeneous population of independent binding sites. Table 2 summarizes, for each

domain, the measured $K_D(IP_6)$ and $K_I(IP_6)$ values, as well as the calculated PIP_n affinity [$K_D(PIP_n)$].

Comparison of the IP_6 affinities of the free PH domains reveals an interesting parallel between the E17K AKT1 PH and PLCδ1 PH domains. These domains share similar IP_6 affinities [$K_D(IP_6)$ values of 11 ± 1 and 3.3 ± 0.2 μM, respectively], in both cases more than 20-fold tighter than that of the WT AKT1 PH domain (260 ± 50 μM) (Table 2). It follows that the E17K charge reversal mutation yields 3.0 RT of additional IP_6 binding free energy under these conditions, making the PIP lipid binding pocket more like that of the PLCδ1 PH domain, at least for the IP_6 ligand.

Comparison of the PH domain affinities for PI(3,4,5)P_3 and PI(4,5)P_2 embedded in synthetic plasma membranes reveals that the E17K mutation triggers a striking change in the PIP lipid selectivity. As previously observed (19,25), the native AKT1 and PLCδ1 PH domains are highly specific for PI(3,4,5)P_3 and PI(4,5)P_2, respectively, and neither domain exhibits measurable affinity for the other target lipid (Table 2). The E17K mutation increases the affinity of the AKT1 PH domain for its target PI(3,4,5)P_3 lipid 7.7-fold (2.0 RT). Even more importantly, it increases the affinity for PI(4,5)P_2 from an unmeasurable level to a level that is easily measured, representing at minimum a 100-fold affinity enhancement ($\gg$4.6 RT). The resulting PI(4,5)P_2 affinity is indistinguishable from that of the PI(4,5)P_2-specific PLCδ1 PH domain [$K_D(PIP_2)$ of 130 ± 30 and 190 ± 70 nM, respectively; the latter agrees well with previously published values for the PLCδ1 PH domain (25), further validating the competitive displacement assay]. Thus, the E17K mutation substantially weakens the specificity of the AKT1 PH domain, converting it from a PI(3,4,5)P_3-specific domain into a PI(3,4,5)P_3- and PI(4,5)P_2-binding domain.

Kinetic Analysis of PIP Lipid On- and Off-Rates

In principle, the E17K mutation could increase the affinity for PI(3,4,5)P_3 and PI(4,5)P_2 by increasing the association rate constant (k_{on}), decreasing the dissociation rate constant (k_{off}), or both. To measure association and dissociation kinetics, we utilized a stopped-flow fluorimeter to rapidly mix reactant solutions while monitoring the approach to equilibrium via protein-to-membrane FRET. The resulting association or dissociation FRET time courses displayed in Figure 3 were best fit as described in Materials and Methods to extract the association and dissociation rate constants summarized in Table 2. These studies compared the kinetics of WT and E17K AKT1 PH domains binding to synthetic plasma membranes containing a single target PIP lipid, either PI(3,4,5)P_3 or PI(4,5)P_2.

Association reactions were carried out by rapidly mixing the free PH domain with target membranes while monitoring the approach to equilibrium (under the saturating conditions employed, the off-rate is negligible and the approach to equilibrium yields the true on-rate). Figure 3A shows that the E17K mutation has only a minor effect on PI(3,4,5)P_3 association kinetics, slowing the on-rate constant for binding to PI(3,4,5)P_3-containing membranes less than 2-fold [k_{on} values of (1.3 ± 0.2) × 10^7 and (2.4 ± 0.2) × 10^7 M^{-1} s^{-1} for the E17K and WT AKT1 PH domains, respectively]. The low affinity of the WT PH domain for PI(4,5)P_2 prevents measurement of an on-rate for this lipid and thus prevents direct analysis of the effect of the E17K mutation on the PI(4,5)P_2 association kinetics. Strikingly, however, the E17K mutant displays virtually identical on-rates for PI(3,4,5)P_3-and PI(4,5)P_2-containing membranes (Figure 3A,B). It follows that the substantial effect of the E17K mutation on the equilibrium PI(3,4,5)P_3 affinity, as well as the different affinities of the E17K mutant for PI(3,4,5)P_3 and PI(4,5)P_2, arises primarily from large differences in dissociation rates (Table 2).

Dissociation reactions were carried out by rapidly mixing preformed PH domain–membrane complexes with excess competitive inhibitor, IP_6, thereby ensuring that dissociation is essentially irreversible. Figure 3C confirms that the E17K mutation slows dissociation of the PH domain from PI(3,4,5)P_3 to a rate 18-fold slower than the native rate (k_{off} values of 0.06 ± 0.01 and 1.1 ± 0.1 s^{-1} for E17K and WT AKT1 PH domains, respectively) (Table 2). Moreover, the dissociation of the E17K mutant from PI(3,4,5)P_3 is 24-fold slower than dissociation from PI(4,5)P_2, verifying that dissociation kinetics dominate affinity.

As a positive control, the measured on- and off-rate constants were used to calculate the corresponding equilibrium dissociation constant [$K_D(PIP_n) = k_{off}/k_{on}$, a calculation that assumes binding and dissociation are simple, one-step reactions without intermediate states]. The good agreement between the measured and calculated (Table 2) values of $K_D(PIP_n)$ supports the accuracy of all the equilibrium and kinetic parameters and provides strong evidence that binding and dissociation each occur in one step without intermediates.

Overall, the in vitro equilibrium and kinetic studies indicate that the E17K mutation significantly alters the target lipid specificity of the AKT1 PH domain, yielding a dramatic increase in affinity for PI(4,5)P_2. Since PI(4,5)P_2 is a constitutive plasma membrane component, this specificity change would be expected to alter the distribution of the PH domain between the cytoplasm and plasma membrane, especially in a resting cell lacking a PI(3,4,5)P_3 signal where the native PH domain would be cytoplasmic and the mutant would be membrane-bound. To further test this picture, the sensitivity of intracellular targeting to the levels of PI(3,4,5)P_3 and PI(4,5)P_2 was examined in live cells.

Effects on Membrane Targeting in Live Cells

The in vitro findings predict that the E17K and WT PH domains will exhibit very different membrane targeting patterns when the plasma membrane levels of PI(3,4,5)P_3 and PI(4,5)P_2 are varied in live cells. We used fluorescence microscopy to analyze the intracellular localizations of the Citrine-AKT1 PH, RFP-AKT1 E17K PH, and CFP-PLCδ1 PH domains, in live, serum-starved NIH 3T3 fibroblasts. A three-color system was employed to enable simultaneous imaging of all three fluorescent fusion proteins in the same cell, both in the resting state and in various stimulated states.

The localizations of the three PH domains in the same resting cell, illustrated in Figure 4, were the same as previously observed (16,29–31). The WT AKT1 PH domain remains in the cytoplasm until attractant stimulation of PI3K activity, which triggers rapid translocation to the plasma membrane while PI(3,4,5)P_3 is being produced by PI3K (Figure 4A). Following treatment with wortmannin to inhibit PI3K and block PI(3,4,5)P_3 production, the WT domain returns to the cytoplasm. By contrast, the E17K AKT1 and PLCδ1 PH domains are are already colocalized to the plasma membrane in the resting state, prior to stimulation (Figure 4A). This constitutive plasma membrane targeting is not due to a low, basal level of PI3K-generated PI(3,4,5)P_3 since it is not disrupted by serum starvation in the presence of a PI3K inhibitor prior to imaging (ref [16] and our data for wortmannin not shown). Instead, the simplest explanation for this constitutive targeting is high-affinity binding to PI(4,5)P_2, a constitutive component of the plasma membrane inner leaflet. The PLCδ1 PH domain is known to exhibit such high-affinity PI(4,5)P_2 binding (25,32,33), and the in vitro results for the E17K AKT1 PH domain indicate it should exhibit similar behavior. Upon stimulation, additional plasma membrane targeting is observed for the E17K AKT1 PH domain, which also binds PI(3,4,5)P_3, but not for the PI(4,5)P_2-specific PLCδ1 PH domain (Figure 4A).

To directly test whether the constitutive colocalization of the E17K AKT1 and PLCδ1 PH domains requires plasma membrane PI(4,5)P_2, we used cytoplasmic Ca^{2+} to activate PLCδ hydrolysis, thereby specifically destroying the plasma membrane PI(4,5)P_2 population

(32,34). Figure 4B shows time-lapse images of the initial colocalization of E17K AKT1 and PLCδ1 PH domains on the plasma membrane in resting, serum-starved cells. Subsequently, following Ca^{2+}-ionomycin treatment to stimulate the entry of Ca^{2+} into the cell, both PH domains rapidly dissociate from the plasma membrane. Such dissociation is not an artifact of the submillimolar Ca^{2+} levels introduced by Ca^{2+}-ionomycin treatment, since a control study shows that millimolar Ca^{2+} levels do not displace either PH domain from the target membrane in vitro (Figure 4C). Instead, the simplest interpretation is that the E17K mutant, like the PLCδ1 PH domain, is localized to the plasma membrane via $PI(4,5)P_2$ binding. When $PI(4,5)P_2$ is destroyed by Ca^{2+}-ionomycin treatment, the two PH domains return to the cytoplasm with essentially the same time courses (Figure 4E). Together, the colocalization of the E17K mutant and PLCδ1 PH domains at the plasma membrane of resting cells, as well as the sensitivity of this colocalization to $PI(4,5)P_2$ hydrolysis and its insensitivity to PI3K inhibitors, indicates that the constitutive plasma membrane targeting of the E17K AKT1 PH domain arises from high-affinity binding to $PI(4,5)P_2$ rather than $PI(3,4,5)P_3$.

DISCUSSION

The recent observation that the E17K mutation is highly oncogenic and targets the AKT1 PH domain constitutively and specifically to the plasma membrane (16) raised important questions about its molecular mechanism of membrane targeting. Our findings provide strong evidence of three conclusions: (i) the E17K mutation broadens the PIP lipid specificity of the AKT1 PH domain by greatly increasing the affinity for $PI(4,5)P_2$, thereby altering membrane targeting in vitro and in live cells; (ii) the modified side chain charge at position 17 is responsible for this PIP specificity change; and (iii) the E17K mutation has little effect on the measured PIP lipid association rates but alters the dissociation kinetics, indicating that the observed changes to equilibrium binding and selectivity arise from effects on the stability of the protein–PIP lipid complex.

Our findings indicate that the E17K mutation significantly alters the equilibrium lipid affinity and specificity of the PIP binding pocket in vitro. This mutation generates a 23-fold increase in affinity for the soluble IP_6 molecule and a 7-fold increase in affinity for the native target lipid $PI(3,4,5)P_3$ (Table 2). Most importantly, however, the mutation also triggers an at least 100-fold increase in the affinity for the constitutive plasma membrane lipid $PI(4,5)P_2$ (Table 2). It is the E17K side chain charge reversal (net charge change of +2) that drives the dramatic $PI(4,5)P_2$ affinity increase; thus, the smaller charge change associated with the E17Q mutation (+1) yields a correspondingly smaller $PI(4,5)P_2$ affinity increase (Figure 1). Strikingly, the $PI(4,5)P_2$ affinity of the E17K mutant [$K_D(PIP_n)$ of 130 ± 30 nM] is nearly identical to that observed for the PLCδ1 PH domain [$K_D(PIP_n)$ of 190 (70 nM], a widely employed specific $PI(4,5)P_2$ sensor (26,29,31). Both of these affinities are sufficient to bind to the physiological concentration of $PI(4,5)P_2$ provided by the plasma membrane [2–10 μM (27,35)]. Further kinetic results indicate that these equilibrium affinity changes stem from the effect of the E17K mutation on the stability of the PH domain–ligand complex. Notably, these in vitro equilibrium and kinetic measurements employed PIP lipids embedded in a synthetic plasma membrane that closely mimics the lipid composition of the native, plasma membrane inner leaflet, thereby maximizing the relevance of the studies to targeting in live cells. Overall, the in vitro results provide a clear physical explanation for the plasma membrane targeting of both domains observed in live cells.

Live cell studies were carried out to test the key conclusion of the in vitro findings, namely, that the E17K charge reversal mutation triggers an increase in $PI(4,5)P_2$ affinity sufficient to drive binding to physiological levels of this lipid in the plasma membrane. Tricolor fluorescence imaging was employed to simultaneously monitor the cellular distribution of

the WT AKT1 PH domain fused to Citrine, the E17K AKT1 PH domain fused to RFP, and the PLCδ1 PH domain fused to CFP. As previously observed (16,29), the WT AKT1 PH domain is cytoplasmic in resting cells and driven to the plasma membrane by a $PI(3,4,5)P_3$ signal, while the E17K AKT1 and PLCδ1 PH domains are constitutively targeted to the plasma membrane in both resting and activated cells. The plasma membrane targeting of the WT AKT1 PH domain in activated cells requires $PI(3,4,5)P_3$ and is thus reversed by PI3K inhibition, while the targeting of the E17K AKT1 and PLCδ1 PH domains is insensitive to this treatment. Instead, both the E17K AKT1 and PLCδ1 PH domains are released from the plasma membrane by hydrolysis of $PI(4,5)P_2$. These live cell findings confirm that the constitutive plasma membrane targeting of the E17K AKT1 PH domain, like that of the control PLCδ1 PH domain, is dominated by binding to the constitutive plasma membrane lipid $PI(4,5)P_2$.

Together, the in vitro and live cell studies indicate that the primary physiological effect of the E17K mutation is to broaden the PIP lipid specificity of the headgroup binding site, generating a large increase in $PI(4,5)P_2$ affinity sufficient to drive constitutive plasma membrane targeting. For full-length AKT1, the enhanced plasma membrane localization driven by the E17K mutation is expected to promote additional AKT1 phosphorylation by the membrane-bound kinase PDK1, thereby explaining the propensity of E17K to trigger constitutive AKT1 activation and oncogenesis.

Finally, we propose a simple molecular model in which the native Glu17 side chain plays a central role in controlling the $PI(3,4,5)P_3$ affinity and specificity of the wild-type PH domain. Since analogous anionic side chains are found in, for example, GRP1 PH and Btk PH (36,37), we predict this model will be able to be generalized to a subset of other $PI(3,4,5)P_3$-specific PH domains. In fact, the E41K mutant of the Btk PH domain is also known to generate constitutive plasma membrane targeting via an unknown mechanism (38): we propose this mutation increases affinity for $PI(4,5)P_2$ in the same manner as E17K in the AKT1 PH domain. Briefly, the native AKT1 PH domain must recognize a small-amplitude $PI(3,4,5)P_3$ signal in the presence of much higher background levels of $PI(4,5)P_2$; thus, the headgroup binding pocket[2] must bind $PI(3,4,5)P_3$ tightly while excluding $PI(4,5)P_2$. We propose that the anionic Glu17 side chain generates unfavorable electrostatic interactions with the anionic phosphates at the 4- and 5-positions of the inositol ring, thereby decreasing the equilibrium affinities of all PIP lipids possessing phosphates at those positions, including $PI(4,5)P_2$ and $PI(3,4,5)P_3$. For the target $PI(3,4,5)P_3$ lipid, this affinity loss is more than offset by a large, favorable electrostatic interaction between the headgroup binding site and the phosphate at the 3-position of the inositol ring, enabling efficient binding to the low levels of $PI(3,4,5)P_3$ generated during signaling events. In this model, the native Glu17 side chain plays essential roles in the exclusion of $PI(4,5)P_2$ from the binding pocket and in the tuning of the native target $PI(3,4,5)P_3$ affinity. When the side chain charge is reversed by the E17K mutation, the favorable electrostatic interaction between the Lys side chain and the PIP anionic phosphates increases the binding pocket affinity for all ligands tested: IP_6, $PI(4,5)P_2$, and $PI(3,4,5)P_3$. This affinity enhancement is at least 10-fold

[2]For the sake of simplicity, it is assumed that $PI(3,4,5)P_3$ and $PI(4,5)P_2$ bind competitively to the same binding pocket. Four lines of evidence support this assumption. (i) A separate, low-affinity binding site for $PI(4,5)P_2$ has been proposed (39) for the closely related AKT2 PH domain, but we do not detect binding of the AKT1 PH domain to membrane-bound $PI(4,5)P_2$ in the absence of $PI(3,4,5)P_3$ (Table 2); thus, it is not clear this isoform possesses a distinct $PI(4,5)P_2$ binding site. (ii) Addition of $PI(4,5)P_2$ to $PI(3,4,5)P_3$-containing membranes has no detectable effect on the membrane affinities of the WT and E17K AKT1 PH domains; thus, the affinity increase expected for simultaneous binding of $PI(3,4,5)P_3$ and $PI(4,5)P_2$ to two distinct sites (39) is not observed (K. E. Landgraf and J. J. Falke, unpublished observations). (iii) IP_6 displaces the E17K mutant both from membrane-associated $PI(3,4,5)P_3$ and from membrane-associated $PI(4,5)P_2$, consistent with a simple model in which IP_6, $PI(3,4,5)P_3$, and $PI(4,5)P_2$ all bind competitively to the same headgroup binding pocket. (iv) The E17K mutation is directly adjacent to the headgroup binding pocket (16) and is considerably more distant from the putative distinct $PI(4,5)P_2$ binding pocket (39). Thus, the strong affinity enhancement triggered by the E17K substitution for $PI(3,4,5)P_3$, and especially for $PI(4,5)P_2$, is easily explained if both headgroups occupy the same binding pocket.

larger, however, for $PI(4,5)P_2$ than for the other two ligands. Thus, we predict that the $PI(4,5)P_2$ headgroup occupies the pocket in an orientation different from that observed in the known structure of the E17K PH–$PI(3,4,5)P_3$ complex (16), placing the inositol 4-and 5-positions of $PI(4,5)P_2$ at a location that enables stronger interactions with the mutant Lys side chain. The resulting, large affinity increase for $PI(4,5)P_2$ is essential to the constitutive plasma membrane targeting of the mutant PH domain and thus to the oncogenic nature of the full-length E17K AKT1 protein.

Acknowledgments

We gratefully acknowledge the gift of the PLCδ1 PH domain from Dr. M. Katan (Cancer Research UK Centre for Cell and Molecular Biology), as well as helpful discussions with Dr. J. H. Evans (University of Colorado).

REFERENCES

1. Vanhaesebroeck B, Leevers SJ, Ahmadi K, Timms J, Katso R, Driscoll PC, Woscholski R, Parker PJ, Waterfield MD. Synthesis and function of 3-phosphorylated inositol lipids. Annu. Rev. Biochem 2001;70:535–602. [PubMed: 11395417]
2. Payrastre B, Missy K, Giuriato S, Bodin S, Plantavid M, Gratacap M. Phosphoinositides: Key players in cell signalling, in time and space. Cell. Signalling 2001;13:377–387. [PubMed: 11384836]
3. Cho W, Stahelin RV. Membrane-protein interactions in cell signaling and membrane trafficking. Annu. Rev. Biophys. Biomol. Struct 2005;34:119–151. [PubMed: 15869386]
4. Lemmon MA, Ferguson KM. Signal-dependent membrane targeting by pleckstrin homology (PH) domains. Bio-chem. J 2000;350(Part 1):1–18.
5. Hurley JH, Meyer T. Subcellular targeting by membrane lipids. Curr. Opin. Cell Biol 2001;13:146–152. [PubMed: 11248547]
6. Hawkins PT, Anderson KE, Davidson K, Stephens LR. Signalling through Class I PI3Ks in mammalian cells. Biochem. Soc. Trans 2006;34:647–662. [PubMed: 17052169]
7. Stephens LR, Hughes KT, Irvine RF. Pathway of phosphatidylinositol(3,4,5)-trisphosphate synthesis in activated neutrophils. Nature 1991;351:33–39. [PubMed: 1851250]
8. Isakoff SJ, Cardozo T, Andreev J, Li Z, Ferguson KM, Abagyan R, Lemmon MA, Aronheim A, Skolnik EY. Identification and analysis of PH domain-containing targets of phosphatidylinositol 3-kinase using a novel in vivo assay in yeast. EMBO J 1998;17:5374–5387. [PubMed: 9736615]
9. Lemmon MA. Pleckstrin homology (PH) domains and phosphoinositides. Biochem. Soc. Symp 2007:81–93. [PubMed: 17233582]
10. Lemmon MA, Ferguson KM. Molecular determinants in pleckstrin homology domains that allow specific recognition of phosphoinositides. Biochem. Soc. Trans 2001;29:377–384. [PubMed: 11497993]
11. Mora A, Komander D, van Aalten DM, Alessi DR. PDK1, the master regulator of AGC kinase signal trans-duction. Semin. Cell Dev. Biol 2004;15:161–170. [PubMed: 15209375]
12. Andrews S, Stephens LR, Hawkins PT. PI3K class IB pathway in neutrophils. Sci. STKE 2007:cm3. [PubMed: 17925574]
13. Manning BD, Cantley LC. AKT/PKB signaling: Navigating downstream. Cell 2007;129:1261–1274. [PubMed: 17604717]
14. Cantley LC, Neel BG. New insights into tumor suppression: PTEN suppresses tumor formation by restraining the phosphoinositide 3-kinase/AKT pathway. Proc. Natl. Acad. Sci. U.S.A 1999;96:4240–4245. [PubMed: 10200246]
15. Hennessy BT, Smith DL, Ram PT, Lu Y, Mills GB. Exploiting the PI3K/AKT pathway for cancer drug discovery. Nat. Rev. Drug Discovery 2005;4:988–1004.
16. Carpten JD, Faber AL, Horn C, Donoho GP, Briggs SL, Robbins CM, Hostetter G, Boguslawski S, Moses TY, Savage S, Uhlik M, Lin A, Du J, Qian YW, Zeckner DJ, Tucker-Kellogg G, Touchman J, Patel K, Mousses S, Bittner M, Schevitz R, Lai MH, Blanchard KL, Thomas JE. A transforming

mutation in the pleckstrin homology domain of AKT1 in cancer. Nature 2007;448:439–444. [PubMed: 17611497]

17. Malanga D, Scrima M, De Marco C, Fabiani F, De Rosa N, De Gisi S, Malara N, Savino R, Rocco G, Chiappetta G, Franco R, Tirino V, Pirozzi G, Viglietto G. Activating E17K mutation in the gene encoding the protein kinase AKT1 in a subset of squamous cell carcinoma of the lung. Cell Cycle 2008;7:665–669. [PubMed: 18256540]
18. Biondi RM, Komander D, Thomas CC, Lizcano JM, Deak M, Alessi DR, van Aalten DM. High resolution crystal structure of the human PDK1 catalytic domain defines the regulatory phosphopeptide docking site. EMBO J 2002;21:4219–4228. [PubMed: 12169624]
19. Frech M, Andjelkovic M, Ingley E, Reddy KK, Falck JR, Hemmings BA. High affinity binding of inositol phosphates and phosphoinositides to the pleckstrin homology domain of RAC/protein kinase B and their influence on kinase activity. J. Biol. Chem 1997;272:8474–8481. [PubMed: 9079675]
20. Andjelkovic M, Alessi DR, Meier R, Fernandez A, Lamb NJ, Frech M, Cron P, Cohen P, Lucocq JM, Hemmings BA. Role of translocation in the activation and function of protein kinase B. J. Biol. Chem 1997;272:31515–31524. [PubMed: 9395488]
21. Bellacosa A, Chan TO, Ahmed NN, Datta K, Malstrom S, Stokoe D, McCormick F, Feng J, Tsichlis P. Akt activation by growth factors is a multiple-step process: The role of the PH domain. Oncogene 1998;17:313–325. [PubMed: 9690513]
22. Alessi DR, James SR, Downes CP, Holmes AB, Gaffney PR, Reese CB, Cohen P. Characterization of a 3-phosphoinositide-dependent protein kinase which phosphorylates and activates protein kinase Bα. Curr. Biol 1997;7:261–269. [PubMed: 9094314]
23. Anderson KE, Coadwell J, Stephens LR, Hawkins PT. Translocation of PDK-1 to the plasma membrane is important in allowing PDK-1 to activate protein kinase B. Curr. Biol 1998;8:684–691. [PubMed: 9637919]
24. Corbin JA, Evans JH, Landgraf KE, Falke JJ. Mechanism of specific membrane targeting by C2 domains: Localized pools of target lipids enhance Ca^{2+} affinity. Biochemistry 2007;46:4322–4336. [PubMed: 17367165]
25. Garcia P, Gupta R, Shah S, Morris AJ, Rudge SA, Scarlata S, Petrova V, McLaughlin S, Rebecchi MJ. The pleckstrin homology domain of phospholipase C-δ1 binds with high affinity to phosphatidylinositol 4,5-bisphosphate in bilayer membranes. Biochemistry 1995;34:16228–16234. [PubMed: 8519781]
26. Varnai P, Balla T. Visualization of phosphoinositides that bind pleckstrin homology domains: Calcium- and gonist-induced dynamic changes and relationship to myo-[^{3}H]inositollabeled phosphoinositide pools. J. Cell Biol 1998;143:501–510. [PubMed: 9786958]
27. Corbin JA, Dirkx RA, Falke JJ. GRP1 pleckstrin homology domain: Activation parameters and novel search mechanism for rare target lipid. Biochemistry 2004;43:16161–16173. [PubMed: 15610010]
28. Evans JH, Falke JJ. Ca^{2+} influx is an essential component of the positive-feedback loop that maintains leading-edge structure and activity in macrophages. Proc. Natl. Acad. Sci. U.S.A 2007;104:16176–16181. [PubMed: 17911247]
29. Varnai P, Balla T. Live cell imaging of phosphoinositide dynamics with fluorescent protein domains. Biochim. Biophys. Acta 2006;1761:957–967. [PubMed: 16702024]
30. Servant G, Weiner OD, Herzmark P, Balla T, Sedat JW, Bourne HR. Polarization of chemoattractant receptor signaling during neutrophil chemotaxis. Science 2000;287:1037–1040. [PubMed: 10669415]
31. Stauffer TP, Ahn S, Meyer T. Receptor-induced transient reduction in plasma membrane PtdIns(4,5)P2 concentration monitored in living cells. Curr. Biol 1998;8:343–346. [PubMed: 9512420]
32. van der Wal J, Habets R, Varnai P, Balla T, Jalink K. Monitoring agonist-induced phospholipase C activation in live cells by fluorescence resonance energy transfer. J. Biol. Chem 2001;276:15337–15344. [PubMed: 11152673]
33. Singh SM, Murray D. Molecular modeling of the membrane targeting of phospholipase C pleckstrin homology domains. Protein Sci 2003;12:1934–1953. [PubMed: 12930993]

34. Allen, Va; Swigart, Pa; Cheung, Ra; Cockcroft, Sa; Katan, Ma. Regulation of inositol lipid-specific phospholipase cdelta by changes in Ca^{2+} ion concentrations. Biochem. J 1997;327(Part 2):545–552. [PubMed: 9359428]

35. Golebiewska U, Nyako M, Woturski W, Zaitseva I, McLaughlin S. Diffusion Coefficient of Fluorescent Phosphatidylinositol 4,5-bisphosphate in the Plasma Membrane of Cells. Mol. Biol. Cell 2008;19:1663–1669. [PubMed: 18256277]

36. Lietzke SE, Bose S, Cronin T, Klarlund J, Chawla A, Czech MP, Lambright DG. Structural basis of 3-phosphoinositide recognition by pleckstrin homology domains. Mol. Cell 2000;6:385–394. [PubMed: 10983985]

37. Baraldi E, Djinovic Carugo K, Hyvonen M, Surdo PL, Riley AM, Potter BV, O'Brien R, Ladbury JE, Saraste M. Structure of the PH domain from Bruton's tyrosine kinase in complex with inositol 1,3,4,5-tetrakisphosphate. Structure 1999;7:449–460. [PubMed: 10196129]

38. Varnai P, Rother KI, Balla T. Phosphatidylinositol-3-kinase dependent membrane association of the Bruton's tyrosine kinase pleckstrin homology domain visualized in single living cells. J. Biol. Chem 1999;274:10983–10989. [PubMed: 10196179]

39. Augin D, Barthe P, Auge-Senegas MT, Stern MH, Noguchi M, Roumestand C. Solution structure and backbone dynamics of the pleckstrin homology domain of the human protein kinase B (PKB/Akt). Interaction with inositol phosphates. J. Biomol. NMR 2004;28:135–155.

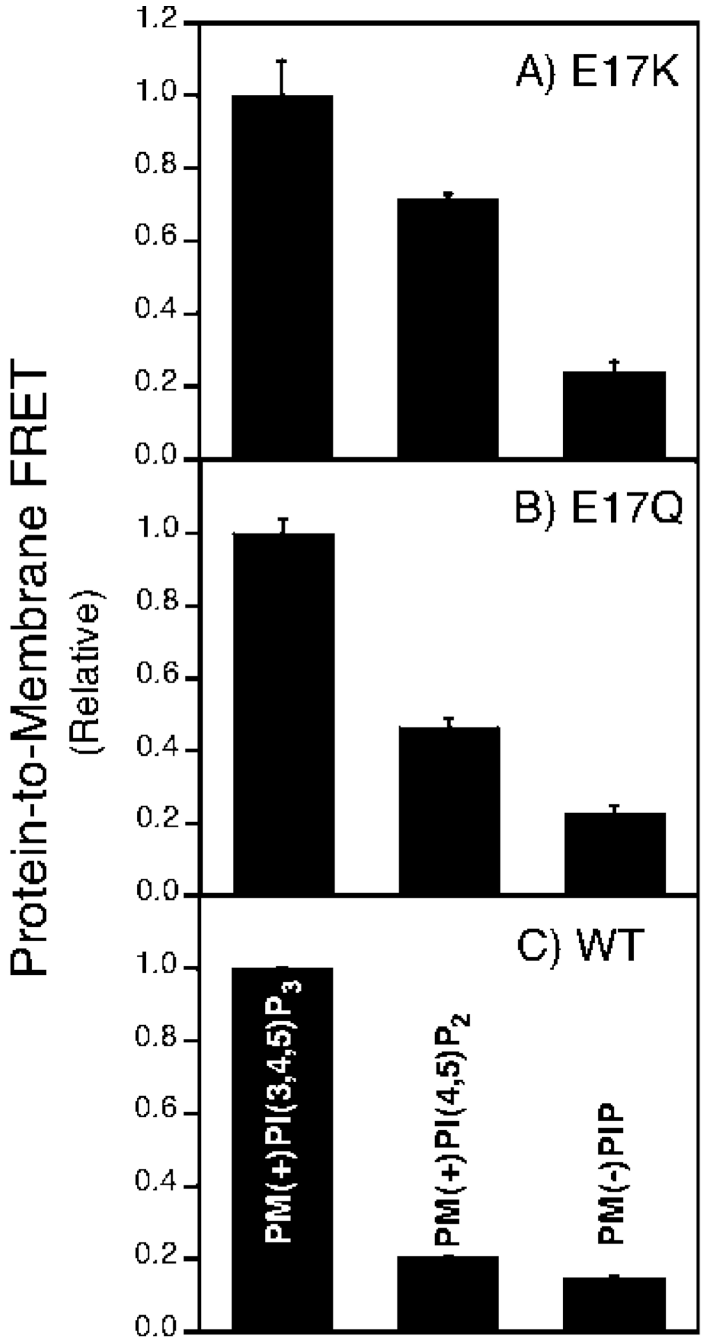

FIGURE 1.

Qualitative PIP lipid specificity assay: (A) AKT1 E17K PH domain, (B) AKT1 E17Q PH domain, and (C) AKT1 PH domain. In all cases, 0.5 μM protein was mixed with 50 μM total membrane lipid, yielding an equimolar ratio of protein to accessible PIP_n target lipid in synthetic plasma membranes [PM(+)PIP_n; see Table 1]. Shown is the average change (±1 standard deviation) in protein-to-membrane FRET upon addition of protein to lipid, measured in at least three independent experiments as described in Materials and Methods.

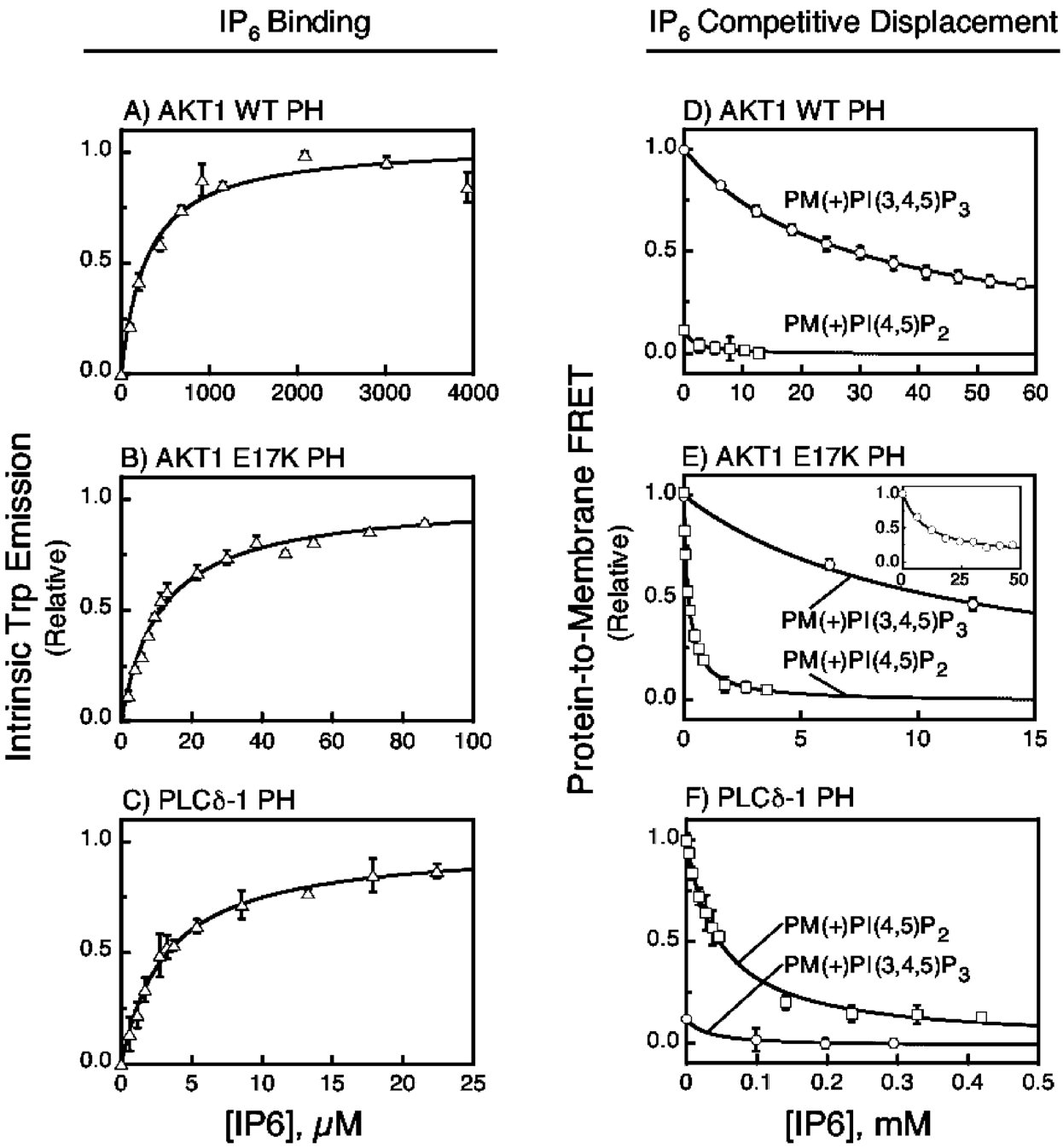

FIGURE 2.

Quantitative equilibrium binding and specificity measurements. (A–C) Direct IP_6 titrations (Δ) of indicated free PH domains. In all cases, 1 μM protein (Materials and Methods) was titrated with IP_6 and the increase in tryptophan emission was measured as described in Materials and Methods. (D–F) Competitive displacement assays performed as described in Materials and Methods for the indicated PH domains bound to synthetic plasma membranes containing either $PI(3,4,5)P_3$ (○) or $PI(4,5)P_2$ (□) (Table 1). In all cases, 0.5 μM protein was mixed with 200 μM total lipid (3 μM accessible PIP_n) and the bound complex was titrated with the competitive inhibitor IP_6. Both the IP_6 binding and competitive displacement assays were carried out in triplicate; data points shown are averages (±1 standard deviation).

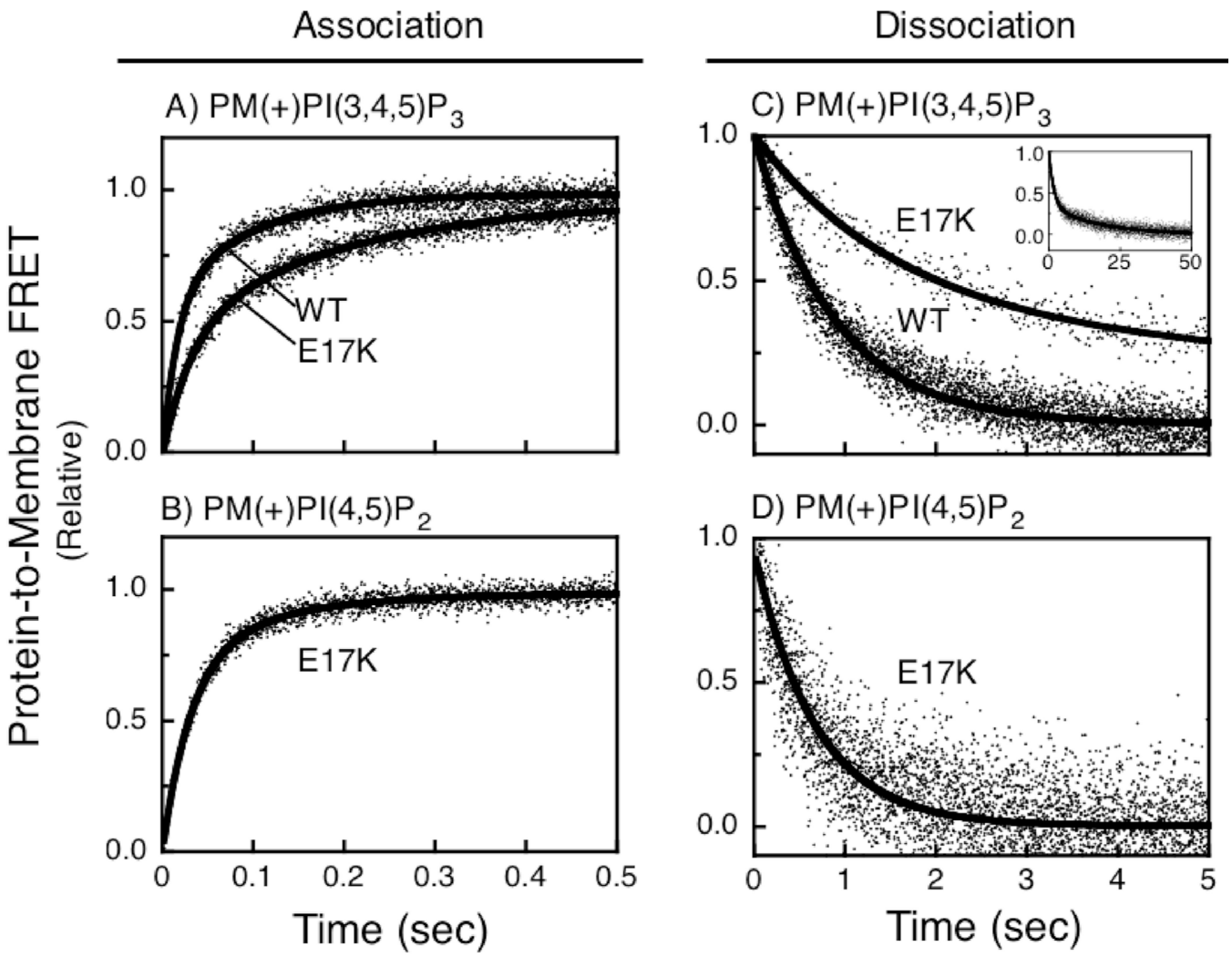

FIGURE 3.

Association and dissociation kinetics. Shown are association reactions (A and B) and dissociation reactions (C and D) for the indicated pairings of the PH domain and PIP lipid embedded in synthetic plasma membranes (Table 1), carried out as described in Materials and Methods. In all cases, protein and lipid concentrations were identical to the equilibrium competitive displacement assays (Figure 2D–F). Reactions were initiated by rapid mixing of either the free PH domain with membranes (association) or the prebound PH domain–membrane complex with 40 mM IP_6 (dissociation). Each data point is a mean value obtained by averaging at least five replicate time courses.

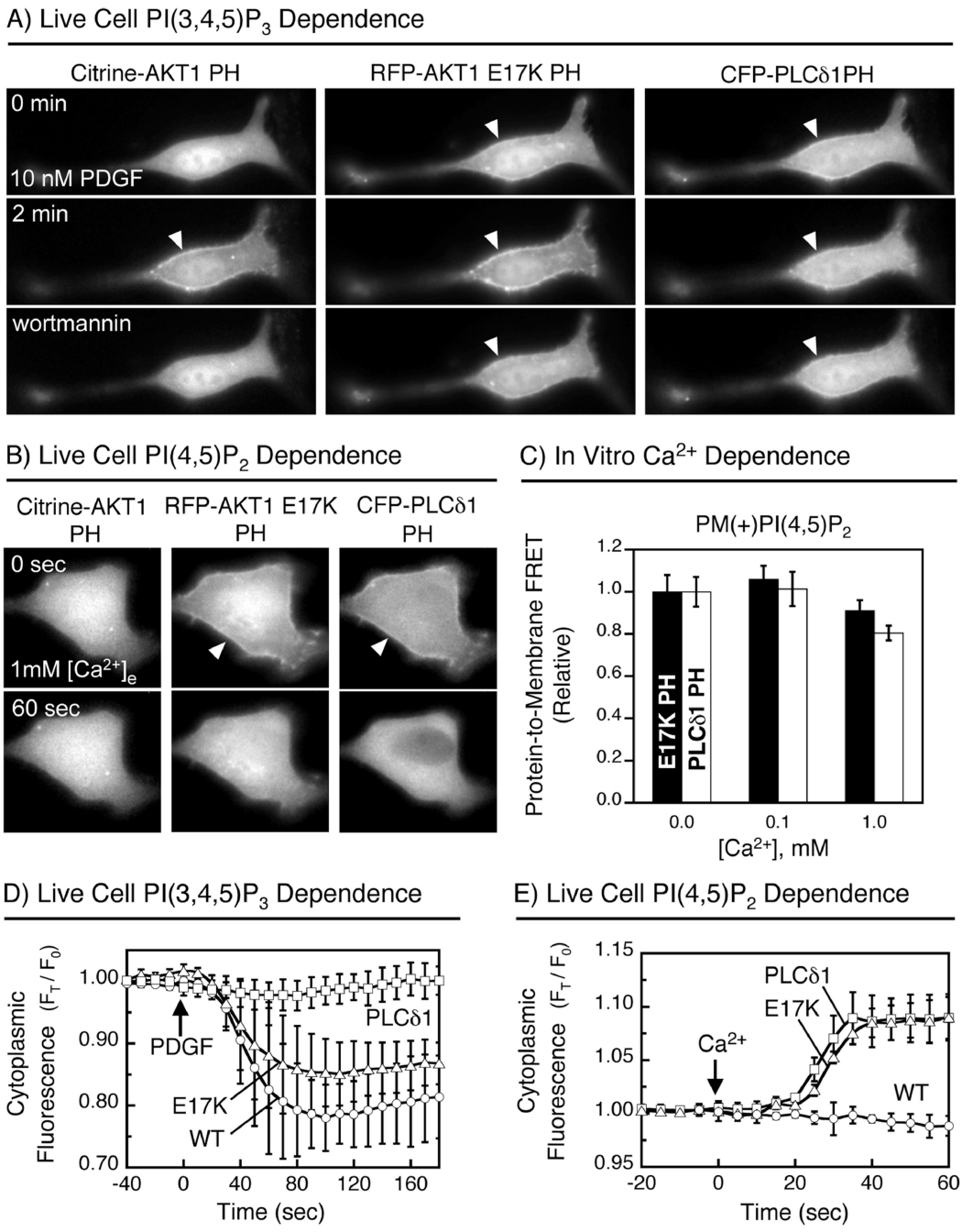

FIGURE 4.

PIP lipid dependence of plasma membrane targeting in NIH 3T3 cells. (A) Dependence of Citrine-AKT1 PH, RFP-AKT1 E17K PH, and CFP-PLCδ1 PH targeting to plasma membrane on $PI(3,4,5)P_3$ production. Serum-starved NIH 3T3 cells were stimulated with 10 nM PDGF and imaged at the indicated times. After 5 min in PDGF, 800 nM wortmannin was added and incubated for 15 min prior to the final image. (B) Dependence of Citrine-AKT1 PH, RFP-AKT1 E17K PH, and CFP-PLCδ1 PH targeting to plasma membrane on $PI(4,5)P_2$. Serum-starved NIH 3T3 cells were incubated with 10 μM ionomycin in Ca^{2+}-free buffer for 5 min and then stimulated with 1 mM extracellular Ca^{2+} to trigger $PI(4,5)P_2$ hydrolysis (26). (C) In vitro dependence of E17K AKT1 and PLCδ1 PH domains binding to

synthetic plasma membranes on Ca^{2+} concentration. (D) Quantitative kinetic analysis of representative PI(3,4,5)P_3-induced plasma membrane binding triggered by attractant PDGF addition (A) comparing the cytoplasmic fluorescence of Citrine-AKT1 PH (○), RFP-AKT1 E17K PH (Δ), and CFP-PLCδ1 PH (□) domains. Where observed, the decrease in cytoplasmic fluorescence results from translocation to the plasma membrane. (E) Quantitative kinetic analysis of representative PI(4,5)P_2 hydrolysis reactions triggered by Ca^{2+}-ionomycin treatment (B) comparing the cytoplasmic fluorescence of Citrine-AKT1 PH (○), RFP-AKT1 E17K PH (Δ), and CFP-PLCδ1 PH (□) domains. Where observed, the increase in cytoplasmic fluorescence results from membrane dissociation. For all experiments, see Materials and Methods for details. Data shown in panels A and B are representative of 15 cells examined; data shown in panel C are the averages of triplicates ± 1 standard deviation. In panels D and E, the data are averages ± 1 standard deviation for three representative cells, illustrating the similar translocation kinetics exhibited by the E17K AKT1 PH and PLCδ1 PH domains despite significant cell-to-cell variability in the magnitudes of translocation-associated fluorescence changes.

Table 1

Lipid Compositions of Synthetic Plasma Membranes Containing PIP Lipids

name	lipid mixture	lipid mole %
PM(+)PIP_n	PE/PC/PS/PI/SM/CH/dPE/PIP_n	28/10/21/4.5/4.5/25/5/2
PM(−)PIP	PE/PC/PS/PI/SM/CH/dPE	30/10/21/4.5/4.5/25/5

Table 2

Equilibrium and Kinetic Parameters for PH Domains Binding to Synthetic Plasma Membranes Containing PIP Lipids

			equilibrium		kinetics		
PH domain	**$K_D(IP_6)$ (μM)**	**lipid mixture**	**$K_I(IP_6)$ (mM)**	**$K_D(PIP_n)$ (nM)**	**k_{on} ($\times 10^7$ M^{-1} s^{-1})**	**k_{off} (s^{-1})**	**K_D (k_{off}/k_{on}) (nM)**
AKT1	260 ± 50	PM(+)PI(3,4,5)P_3	28 ± 1	23 ± 6	2.4 ± 0.2	1.1 ± 0.1	46 ± 6
		PM(+)PI(4,5)P_2	ND[a]	>10^4[b]	–	–	–
AKT1 E17K	11 ± 1	PM(+)PI(3,4,5)P_3	8±2	3 ± 1	1.3 ± 0.2	0.06 ± 0.01	5 ± 1
		PM(+)PI(4,5)P_2	0.21 ± 0.01	130 ± 30	1.3 ± 0.1	1.5 ± 0.1	120 ± 10
PLCδ1	3.0 ± 0.2	PM(+)PI(3,4,5)P_3	ND[a]	>10^4[b]	–	–	–
		PM(+)PI(4,5)P_2	0.047 ± 0.004	190 ± 70	–	–	–

[a] Binding too weak for the competitive assay.

[b] The indicated $K_D(PIP_n)$ is the lower limit of the dissociation constant.